

Determination of irreversibility fields and superconducting parameters in $\text{BaPb}_{0.75}\text{Bi}_{0.25}\text{O}_3$

D. N. Zheng and Z. X. Zhao

*National Laboratory for Superconductivity, Institute of Physics, Chinese Academy of Sciences,
Beijing 100080, People's Republic of China*

A. M. Campbell

*Interdisciplinary Research Center in Superconductivity, University of Cambridge, Madingley Road,
Cambridge CB3 0HE, United Kingdom*

(Received 17 August 1999; revised manuscript received 1 December 1999)

The dc magnetization of a superconducting $\text{BaPb}_{0.75}\text{Bi}_{0.25}\text{O}_3$ sample has been measured as a function of magnetic field and temperature. The results showed that an irreversibility line lies considerably below the superconducting normal phase transition boundary $B_{c2}(T)$, similar to that commonly observed in high-temperature superconductors, even though $\text{BaPb}_{0.75}\text{Bi}_{0.25}\text{O}_3$ displays a very long coherence length. We attributed the observed large magnetically reversible region to a very small thermodynamic field, which leads to low condensation energies. The reversible magnetization data obtained in the region above the irreversibility line enable us to determine a full set of superconducting parameters for the material.

I. INTRODUCTION

The oxide superconductor $\text{Ba}(\text{Pb}_{1-x}\text{Bi}_x)\text{O}_3$ has attracted considerable attention because of its interesting superconducting properties. Superconductivity in this system occurs on the border of metal-semiconductor transition, in the composition range $0 < x < 0.35$ with the maximum transition temperature T_c about 13 K ($x \sim 0.25$).^{1,2} One of the intriguing features that this system exhibits is its relatively high superconducting transition temperature despite very low carrier concentration and density of states at the Fermi level.³ In contrast to high-temperature superconducting copper oxides, $\text{Ba}(\text{Pb}_{1-x}\text{Bi}_x)\text{O}_3$ has a simple perovskite-type structure with isotropic structure and without containing any transition-metal elements. Thus a magnetic mechanism may not be expected for the superconductivity in the compound. The superconducting coherence length of the compound is large compared to that of high-temperature cuprates. This is of particular interest for the study of flux pinning and critical current properties, since it has been suggested that the short coherence length is one of the primary factors that leads to the existence of the irreversibility line and weak links at grain boundaries in high-temperature superconductors. The unusual behavior of high-temperature superconductors in the mixed state has attracted considerable attention.⁴ One of the most intriguing phenomena is the existence of the so-called irreversibility line in the field-temperature (B - T) plane. This line separates the B - T plane into two regions: a magnetically reversible one at high temperatures and fields and an irreversible one at low temperatures and fields. It is now well established that the phenomenon results from a complex scenario including very weak electronic coupling between the superconducting CuO_2 layers (which leads to very large anisotropy), short coherence length, and high working temperatures. Therefore, it is believed that the reversible flux motion region in low-temperature superconductors would be too small to be easily observed and would not be of any significance. Little work had been made to investigate the revers-

ible motion of flux lines for low-temperature superconductors before the recognition of the irreversibility line in high-temperature superconductors except for some specially prepared quasi-two-dimensional films.⁵⁻⁷ In 1991, Suenaga *et al.* reported experimental observation of the irreversibility line in commercial superconducting NbTi and Nb_3Sn wires.⁸ They found that these materials have a clear irreversibility line which is substantially lower than the superconducting $B_{c2}(T)$ phase line. They also found their B_{irr} data fitted well to a flux-line-lattice melting line formulated by Houghton, Pelcovits, and Sudbø,⁹ and thus they interpreted the observed irreversibility line as a melting line of the flux-line lattice. Schmidt, Israeloff, and Goldman¹⁰ investigated the irreversibility line of pure Nb film samples following a similar procedure. They compared their experimental data with different models and concluded that the irreversibility line in Nb is also the flux-line-lattice melting line. In other low-temperature superconducting materials, the irreversibility line has also been observed.¹¹⁻¹⁴ For the superconducting oxide $\text{BaPb}_{0.75}\text{Bi}_{0.25}\text{O}_3$, the low carrier concentration and low density of states at the Fermi level should result in a low superconducting condensation energy and a large magnetic penetration depth. This can have considerable effects on flux pinning since the pinning energy is proportional to the condensation energy and the penetration depth provides a measure of the interaction distance of flux lines. In this paper, we report magnetization measurement results on a $\text{BaPb}_{0.75}\text{Bi}_{0.25}\text{O}_3$ sample and show a well-identified irreversibility line in this system. Furthermore, by measuring the reversible magnetization carefully and employing the Ginzburg-Landau relations, we were able to obtain a set of superconducting parameters, such as the critical fields, the coherence length, and the penetration depth for the material. The parameters are of considerable interest for the understanding of superconductivity in the system.

II. EXPERIMENT

The $\text{BaPb}_{0.75}\text{Bi}_{0.25}\text{O}_3$ sample was prepared by a solid-state reaction method. Phase purity was checked by x-ray diffrac-

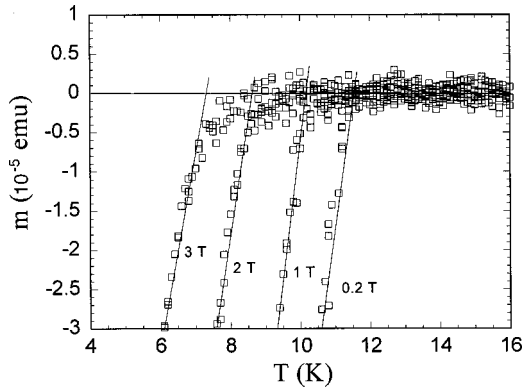


FIG. 1. Zero-field-cooled magnetic moment data as a function of temperature and field.

tion for the sample, and no impurity phases were detected within the sensitivity of the experiment. Bar-shaped sintered samples of dimensions $1 \times 1 \times 6 \text{ mm}^3$ were used in magnetization measurements which were performed on a vibrating sample magnetometer with the applied field parallel to the longest dimension of the sample. For hysteresis loop measurements a field ramp rate 5 mT/s was used. A 10-min delay was introduced prior to each measurement to ensure temperature stabilization. Magnetic relaxation measurements were performed at 4.2 K and 1 T. The field was increased slowly to the required value at 1 mT/s in order to prevent the magnet from overshooting, and the magnetization data were taken about 1 s afterward.

III. RESULTS AND DISCUSSION

As we shall show later in Table I, the coherence length is about 4–30 times larger than that of $\text{YBa}_2\text{Cu}_3\text{O}_7$ (depending on the crystal orientation) and is larger than the width of the structurally disordered region ($\sim 0.5\text{--}2 \text{ nm}$). This together with its isotropic structure makes $\text{BaPb}_{0.75}\text{Bi}_{0.25}\text{O}_3$ an interesting and a comparison model for the study of the weak-link behavior in superconducting ceramic samples that is universally seen in high-temperature superconductors. It has been suggested^{15,16} that in high-temperature cuprates suppression of the superconducting order parameter over a grain boundary “width” comparable to or larger than the coherence length (for $\text{YBa}_2\text{Cu}_3\text{O}_7$: $\xi_{ab} \sim 1\text{--}2 \text{ nm}$, $\xi_c \sim 0.2\text{--}0.4 \text{ nm}$) and crystal lattice misorientations are responsible for the poor coupling between grains that leads to very low polycrystalline transport critical current densities. However, sintered polycrystalline $\text{BaPb}_{0.75}\text{Bi}_{0.25}\text{O}_3$ appears to show evidence of weak-link behavior in a fashion similar to that of polycrystalline high temperature cuprates.¹⁷ In particular, it has been shown that superconductor-insulator-superconductor (SIS) type weak links existed at grain boundaries due to an excess of Pb and Bi.¹⁸ Thus we might conclude that the data we measured represent the properties within grains.

Zero-field-cooled magnetic moment data are shown in Fig. 1 as a function of temperature and magnetic field for the $\text{BaPb}_{0.75}\text{Bi}_{0.25}\text{O}_3$ sample. It can be seen that the magnetic moment varies linearly with temperature for each value of applied field in the superconducting state. The superconducting transition temperature is defined as the intercept of a

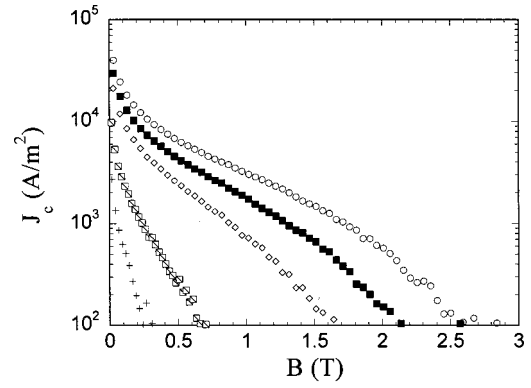


FIG. 2. Critical current density J_c as a function of magnetic field and temperature. From top to bottom the temperatures are 5, 6, 7, 9, and 10 K.

linear extrapolation of the magnetic moment in the superconducting state with the normal-state base line. It is clearly shown in the figure that the transition temperature decreases with increasing magnetic field.

Magnetic hysteresis curves have been measured at several temperatures. The critical current density J_c was calculated from the magnetic hysteresis data using the Bean model.¹⁹ Assuming grains are spherical,

$$J_c (\text{A/m}^2) = 3\Delta M/d, \quad (1)$$

where ΔM (A/m) is the difference in magnetization for increasing and decreasing field, and d (m) is the diameter of the grains. The grain size is about $5 \mu\text{m}$ for our sample. The magnetic field dependence of J_c for different temperatures is shown in Fig. 2.

A moment versus field (m - B) loop measured at 9 K is shown in Fig. 3. The background contribution has been subtracted from the data. Magnetic hysteresis Δm versus the applied field is also plotted in this figure. The irreversibility field B_{irr} is determined as the field above which Δm becomes undetectable, as indicated in the plot. In the reversible region, J_c is less than 10^5 A/m^2 and is below the resolution of the instrument. The upper critical field B_{c2} can also be obtained from the data by extrapolating the reversible magnetization to the $m=0$ line, and the values are in agreement

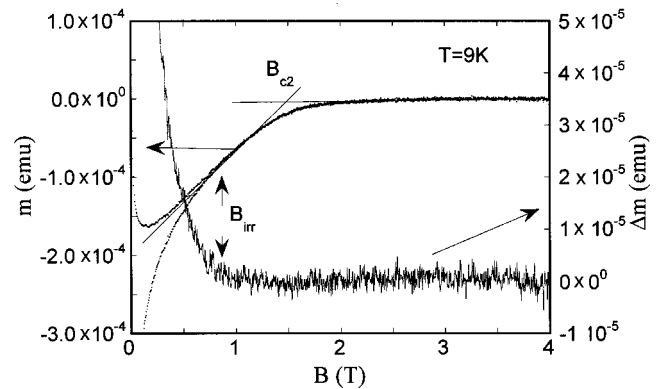


FIG. 3. Magnetic hysteresis curve measured at 9 K. The magnetic hysteresis Δm extracted from the curve is also plotted against the applied field. The upper critical field B_{c2} and the irreversibility field B_{irr} are indicated.

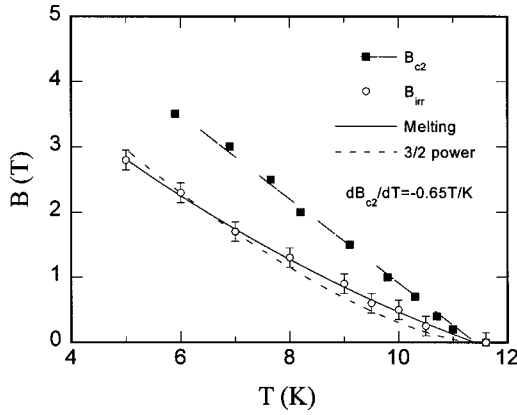


FIG. 4. Temperature dependence of B_{c2} and B_{irr} . The dashed line represents the fit to the thermal depinning line Eq. (4), while the solid line is the fit to the flux-line-lattice melting line, Eq. (5).

with those determined from the m - T curves. The experimental data of B_{c2} and B_{irr} are presented in Fig. 4.

As expected, B_{c2} increases linearly with decreasing temperature with a slope of -0.65 T/K. The zero-temperature value of this parameter $B_{c2}(0)$ is estimated using the formula²⁰

$$B_{c2}(0) = -0.7 \partial B_{c2} / \partial T|_{T_c}. \quad (2)$$

Application of Eq. (1) to the experimental data yields a value of 5.2 T for $B_{c2}(0)$. In addition, in the field region between B_{irr} and B_{c2} , we may apply the theory of Abrikosov²¹ to the reversible magnetization data, the linear part in Fig. 3 is described by

$$-\mu_0 M = (B_{c2} - B) / [\beta_A (2\kappa^2 - 1)]. \quad (3)$$

Here β_A is a constant and is equal to 1.06 for a triangular flux-line lattice, and κ is the Ginzburg-Landau parameter. Using the data collected at 9, 10, and 10.5 K, the value of κ at each temperature was calculated and the averaged value was found to be $\kappa \sim 106$, which is very close to the calculated value based on a single-band model.²² Other superconducting parameters can be calculated by using the Ginzburg-Landau relations: From $B_{c2} = \sqrt{2}\kappa B_c$ and $B_{c1} = B_c (\ln \kappa + 0.5) / (\sqrt{2}\kappa)$, the initial slope of B_c and B_{c2} is found to be -4.6 and -0.17 mT/K, respectively. For B_c , the zero-temperature value is obtained by using the BCS expression $B_c = 1.74 B_c(0) [1 - T/T_c]$, which gives $B_c(0) = 31$ mT. Since there is no theoretical expression for the temperature dependence of B_{c1} , a reasonable approximation to obtain $H_{c1}(0)$ is to use the empirical relation $B_{c1}(T) = B_{c1}(0) [1 - (T/T_c)^2]$. This in turn yields $B_{c1}(0) = 0.97$ mT. Then using relations $B_{c2} = \Phi_0 / (2\pi\xi^2)$, $\xi(T) = \xi(0) [1 - T/T_c]^{-1/2}$, and $\kappa = \lambda(0)/\xi(0)$, the coherence length and penetration depth are calculated to be $\xi(0) = 6.6$ nm and $\lambda(0) = 700$ nm, respectively. Values of these parameters at $T=0$ are listed in Table I. They are, again, in agreement with those

reported in Ref. 17. In particular, our results are in good agreement with the values obtained on single-crystal samples.^{3,23,24} The very large κ value means that the material is an extreme type-II superconductor. It is worthy to point out that unlike high-temperature cuprates $\text{BaPb}_{0.75}\text{Bi}_{0.25}\text{O}_3$ is an extreme Pippard superconductor. The ratio ξ_0/l is estimated to be 10^2 ,²² here, l is the mean free path length and ξ_0 is the BCS coherence length. Therefore, the magnetic field penetration depth λ is expected to be significantly greater than the London penetration depth λ_L and does not provide a direct measure of the superconducting carrier density. Nevertheless, the large penetration depth can be qualitatively explained by the low carrier concentration. The results also show a rather low thermodynamic field value for $\text{BaPb}_{0.75}\text{Bi}_{0.25}\text{O}_3$ [$B_c \sim 0.3$ T for NbTi (Ref. 8) and 1.1 T for $\text{YBa}_2\text{Cu}_3\text{O}_7$ (Ref. 25)]. This is resulted from a rather low density of states at the Fermi level in this material. In the framework of the BCS theory, the electronic specific-heat coefficient γ is related to the critical fields via the relations $\gamma T_c^2 = 1.7 \times 10^6 B_c^2$ or $dB_{c2}/dT = 4.48 \times 10^3 \rho \gamma$ (in SI units). The results obtained from the two relations are consistent and give a γ of 0.5 mJ/mol K² ($\rho \sim 11 \mu\Omega \text{ m}$,²³ while using the second relation), corresponding to a density of states value 0.17 states/f.u. eV spin. The density of states is very small in $\text{BaPb}_{0.75}\text{Bi}_{0.25}\text{O}_3$, and in comparison to T_c of elements or intermetallic compounds, the transition temperature in this oxide superconductor is 3 times higher.²⁶

The data presented in Fig. 4 illustrate a rather large field and temperature range of reversible flux motion in $\text{BaPb}_{0.75}\text{Bi}_{0.25}\text{O}_3$. In fact, it is as large as $\sim 2/3$ of that for $\text{YBa}_2\text{Cu}_3\text{O}_7$ in the same range of reduced temperature (T/T_c) and reduced field [$B/B_{c2}(0)$]. It is well known that the irreversibility line in high-temperature cuprates originates from short coherence lengths, large anisotropy, and high transition temperatures. The irreversibility line observed in low-temperature superconductors is either very close to the transition line, leaving a very small reversible region, or shown in materials having short coherence length like the Chevrel phase superconductor PbMo_6S_8 .¹³ For $\text{BaPb}_{0.75}\text{Bi}_{0.25}\text{O}_3$, therefore, the large reversible region is, at first sight, somewhat surprising since it has a low T_c , a long coherence length, and a cubic structure. However, we note that the thermodynamic field B_c is very low for this material as shown in Table I. At a more fundamental level, the irreversibility line is the manifestation of the interplay between quenched disorder of the flux-line lattice (due to flux pinning) and thermal fluctuations. It has been pointed out⁴ that the fundamental parameter governing the strength of thermal fluctuations is the Ginzburg number $G_i = [k_B T_c / B_c^2(0) \varepsilon \xi^3(0)]^2 / 2$ (here $\varepsilon = (M_z/M)^{1/2}$ is the square root of the ratio of the out-of-plane and in-plane effective masses) which measures the relative size of the minimal ($T=0$) condensation energy $B_c^2(0) \varepsilon \xi^3(0)$ within a coherence volume and the critical temperature T_c . With

TABLE I. Superconducting parameters of $\text{BaPb}_{0.75}\text{Bi}_{0.25}\text{O}_3$.

T_c (K)	κ	B_{c2} (b)	B_{c1} (mT)	B_c (mT)	λ (nm)	ξ (nm)
11.6	106	5.2	0.97	31	700	6.6

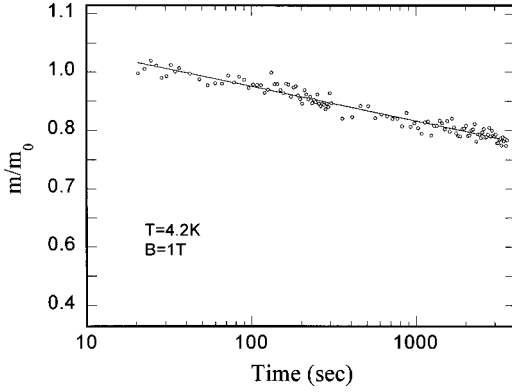


FIG. 5. Magnetic relaxation data taken at 4.2 K and 1 T.

increasing Ginzburg number G_i , the thermal fluctuation region and those parts of the B - T phase diagram where flux motion is reversible become larger. We can calculate G_i for $\text{BaPb}_{0.75}\text{Bi}_{0.25}\text{O}_3$ as well as for some other superconductors such as high-temperature oxide $\text{YBa}_2\text{Cu}_3\text{O}_7$, low-temperature metallic alloy NbTi , and Chevrel phase PbMo_6S_8 using the parameters in Table I and in Refs. 25, 8, and 13. The results show that the G_i value of $\text{BaPb}_{0.75}\text{Bi}_{0.25}\text{O}_3$ is of the same order as $\text{YBa}_2\text{Cu}_3\text{O}_7$, but several orders of magnitude higher than other low-temperature superconductors, indicating large thermal fluctuations. Furthermore, flux pinning is weak in $\text{BaPb}_{0.75}\text{Bi}_{0.25}\text{O}_3$. The pinning energy is proportional to B_c^2 . Hence small B_c means small pinning energy and weak flux pinning. The ratio of the critical current density J_c to the depairing current density J_{c0} ($\sim B_c/\mu_0\lambda$) is a measure of the strength of the pinning. For our sample, we found $J_c/J_{c0} \sim 10^{-3}$, which is much smaller than the ratio for materials like NbTi . Thus the low irreversibility line in $\text{BaPb}_{0.75}\text{Bi}_{0.25}\text{O}_3$ can be qualitatively explained by the strong thermal fluctuations and weak pinning.

The small pinning energy is also apparent from magnetic relaxation measurements. Figure 5 shows data taken at 4.2 K with an applied field of 1 T. The equilibrium magnetization, calculated as an average of the magnetization of increasing and decreasing field, has been subtracted from the data. Despite a relatively large noise level, the data follow a logarithmic relation well. The effective pinning energy U_0 is found to be 12 meV from a fit of the data shown in Fig. 5 to the relation $M(t) = M(0)[1 - (k_B T/U_0) \ln t]$. This value is comparable to that of $\text{YBa}_2\text{Cu}_3\text{O}_7$.²⁷

A simple explanation for the irreversibility line is based upon the thermal depinning theory put forward by Yeshuran and Malozemoff.²⁸ In this model, it is suggested that the irreversibility line is caused by thermally activated depinning process of the flux lines. They assumed that the pinning energy scales as $U_0 \propto B_c^2 a_0^2 \xi$, where $a_0 = 1.075(\Phi_0/B)^{1/2}$ is the flux line lattice spacing. The standard Ginzburg-Landau results $B_c \propto (1-t)$ and $\xi \propto (1-t)^{-1/2}$ then led them to $U_0 \propto (1-t)^{3/2}/B$, where $t = T/T_c$. By combining this temperature dependence of the pinning energy with the thermal-activation-dependent critical current, $J_c = J_{c0}[1 - (k_B T/U_0) \ln(Br\Omega)]$, from Ref. 29, and requiring that the critical current be zero, they obtained a power-law relation to describe the irreversibility line:

$$B_{\text{irr}}(T) = B_0(1 - T/T_c)^{3/2}. \quad (4)$$

Here J_{c0} is the critical current density in the absence of thermal activation, r is the distance between pinning centers, Ω is the oscillation frequency of a flux line inside a pinning well, and E_c is the minimum measurement voltage per meter. The logarithm is typically about 30 (Refs. 28 and 29) and is considered constant for the purposes of their derivation.

We use this equation to fit our data, and the fitted curve is represented by the dashed line in Fig. 4. As shown in the figure, within the experimental error bar the fit of the experimental data to Eq. (4) is good, but not as good as the melting line, which we will discuss later. In deriving Eq. (4), it was assumed that the flux bundle volume contains one power of the coherence length ξ and two powers of the flux lattice spacing a_0 . We relax this assumption and allow an unknown power d of the coherence length, and assume U_0 scales as $U_0 \propto B_c^2 a_0^{3-d} \xi^d$. This leads to $U_0 \propto (1-t)^{2-d/2}/B^{(3-d)/2}$ and $B_{\text{irr}} \propto (1-t)^{(4-d)/(3-d)}$. Then we find that the best fit power law for the irreversibility line results in an exponent 1.28, which leads to the nonsensical result $d \sim -0.6$. On the other hand, according to the thermal depinning model, the magnitude of B_{irr} depends on the time scale of the measurements, moving down for slower measurements. At 4.2 K we performed magnetic hysteresis measurements with three different field sweep rates 20, 7, and 2 mT/s. We found that B_{irr} decreased approximately 0.1 T when the sweep rate was reduced from 20 to 2 mT/s. This change is small and of the same order of the error bar of B_{irr} . Nevertheless, the dependence of B_{irr} on the field sweep rate indicates, at least qualitatively, the thermal depinning nature for the irreversibility line we obtained.

In the work of Suenaga *et al.*⁸ and Schmidt *et al.*,¹⁰ the irreversibility line observed in NbTi , Nb_3Sn and Nb was compared with the flux-line-lattice melting theory of Houghton, Pelcovits, and Sudbø⁹ and surprisingly good data fitting was found. In this theory, the authors found that nonlocal effects (i.e., the finite wave-vector-dependent moduli) are crucial when dealing with compounds where κ is large, as it is in $\text{BaPb}_{0.75}\text{Bi}_{0.25}\text{O}_3$. Specifically, they found that moduli are significantly softer than they would be in a purely local theory. For example, in the local limit, c_{66} vanishes at $B = B_{c2}$ whereas c_{44} and c_{11} achieve their maximum values at the upper critical field. However, the lattice softens significantly in the nonlocal case and all moduli vanish at $B = B_{c2}$. Flux lines tilt easily when c_{44} becomes small as a result of thermal fluctuations. The authors deduced the mean-square displacement of a flux lattice due to thermal fluctuations from the nonlocal moduli and used the Lindermann criterion to estimate the melting line of the flux line lattice. Their melting line is given by

$$\frac{t}{\sqrt{1-t}} \frac{\sqrt{b}}{1-b} \left(\frac{4(\sqrt{2}-1)}{\sqrt{1-b}} + 1 \right) = \alpha, \quad (5)$$

where α measures the degree of susceptibility to thermal motion and is given by

$$\alpha = 2 \times 10^3 \left(\frac{c}{\kappa} \right)^2 \left(\frac{B_{c2}(0)}{T_c^2} \frac{M}{M_z} \right)^{1/2}. \quad (6)$$

Here $t = T/T_c$, $b_m = B_{\text{irr}}/B_{c2}$. The Lindemann criterion for melting is governed by the parameter c , which is the ratio of the mean-square thermal displacement of the flux-line lattice from their equilibrium positions to the flux-line-lattice spacing.

The solid line in Fig. 4 is a single parameter fit of Eq. (5) to the measured irreversibility line data. Within the experimental error bar, it can be seen that the theoretical melting line fits experimental data well. Since M_z/M equals 1 in the case of $\text{BaPb}_{0.75}\text{Bi}_{0.25}\text{O}_3$, we can estimate the Lindemann criterion c . Combining κ with the curve fit value for the parameter α gives $c = 0.066$ for our sample. This value is very similar to that observed by Suenaga *et al.* for NbTi and Nb_3Sn Ref. 8 and is reasonable since values for the melting of an atomic lattice are approximately 0.1.

Although the irreversibility line data reported here and those in Refs. 8 and 10 fit the flux lattice melting theory well, there is a lack of direct evidence to show unambiguously that flux-line-lattice melting can be observed in these materials. For a flux-line-lattice melting transition, we expect abrupt changes in resistivity, susceptibility, magnetization, and anomalies in calorimetric measurements as have been illustrated in some clean high- T_c superconductors.^{30–35} For low- T_c superconductors, to our knowledge only NbSe_2 shows a clear sign of flux-lattice melting.³⁶

The relation between the irreversibility and melting lines is still an issue of current debate. In some reports, the irreversibility line coincides with the melting line,^{37,38} while in some other reports the two lines appear to be uncorrelated.^{33,39} It has been suggested that in high-temperature cuprates the melting line could be the upper limit of the irreversibility line. If flux creep is suppressed by, for example, applying a weak transverse ac magnetic field,⁴⁰ then the two lines coincide with each other.

Finally, we would like to point out that it is difficult to conclude which of the two models discussed above explains the nature of the irreversibility line in $\text{BaPb}_{0.75}\text{Bi}_{0.25}\text{O}_3$ merely based on the fitting in Fig. 4. In particular, we should also take the experimental uncertainty in determining B_{irr} into account. Nevertheless, we want to emphasize that the very low B_c is a major factor that leads to the very low irreversibility line for $\text{BaPb}_{0.75}\text{Bi}_{0.25}\text{O}_3$ regardless of the exact mechanism of the irreversibility line. This is further supported by the following results.

The upper critical field and the irreversibility line of another superconducting oxide LiTi_2O_4 have also been measured. From the results, an irreversibility line was identified too. The results show that the irreversible region is smaller than that observed in the $\text{BaPb}_{0.75}\text{Bi}_{0.25}\text{O}_3$ sample. This is probably because LiTi_2O_4 has a higher density of states,²⁶ which leads to a large condensation energy compared with $\text{BaPb}_{0.75}\text{Bi}_{0.25}\text{O}_3$. In a recent work, Babic *et al.*⁴¹ measured the irreversibility line on the same $\text{YBa}_2\text{Cu}_3\text{O}_{7-\delta}$ single crystal with a range of different δ values and compared their B_{irr} data with $B_c(0)$ data for the same range of δ value obtained in specific-heat measurements. The comparison revealed a striking similarity between these two quantities, showing the close mutual relation between the “strength” of superconductivity $B_c^2(0)$ and the irreversibility field. They concluded that the condensation energy predominantly determines the magnitude of the irreversibility line of $\text{YBa}_2\text{Cu}_3\text{O}_{7-\delta}$ over a significant range of δ . Their results are in agreement with the conclusion we draw here.

In summary, we have performed systematic magnetization measurements on polycrystalline $\text{BaPb}_{0.75}\text{Bi}_{0.25}\text{O}_3$. An irreversibility line $B_{\text{irr}}(T)$, which is significantly lower than the superconducting phase transition line $B_{c2}(T)$, is identified for the material. Large magnetization relaxation has also been observed with a rate similar to that of $\text{YBa}_2\text{Cu}_3\text{O}_7$. A set of superconducting parameters, including the critical fields, the coherence length ξ , the penetration depth λ , and the Ginzburg-Landau parameter κ has been evaluated using reversible magnetization data for $\text{BaPb}_{0.75}\text{Bi}_{0.25}\text{O}_3$. We attribute the existence of the wide magnetic reversible region and the pronounced flux creep effects to the very low thermodynamic field of the material, which results from its low density of states at the Fermi level.

ACKNOWLEDGMENTS

We would like to thank D. S. Sinclair for the preparation of the samples. This work was supported by the K. C. Wong Education Foundation, Hong Kong, the National Center for Research and Development on Superconductivity of China and Engineering and Physical Sciences Research Council, UK.

¹A. W. Sleight, J. L. Gillson, and P. E. Bierstedt, *Solid State Commun.* **17**, 27 (1975).

²T. D. Thanh, A. Koma, and S. Tanaka, *Appl. Phys.* **22**, 205 (1980).

³B. Batlogg, *Physica B* **126**, 275 (1984).

⁴G. Blatter, M. V. Feigel'man, V. B. Geshkenbeih, A. I. Larkin, and V. M. Vinokur, *Rev. Mod. Phys.* **66**, 1125 (1994).

⁵P. L. Gammel, A. F. Hebard, and D. J. Bishop, *Phys. Rev. Lett.* **60**, 144 (1988).

⁶J. M. Graybeal and M. R. Beasley, *Phys. Rev. Lett.* **56**, 173 (1986).

⁷P. Berghuis, A. L. F. van der Slot, and P. H. Kes, *Phys. Rev. Lett.* **65**, 2583 (1990).

⁸M. Suenaga, A. K. Ghosh, Y. Xu, and D. O. Welch, *Phys. Rev. Lett.* **66**, 1777 (1991).

⁹A. Houghton, R. A. Pelcovits, and S. Sudbø, *Phys. Rev. B* **40**, 6763 (1989).

¹⁰M. F. Schmidt, N. E. Israeloff, and A. M. Goldman, *Phys. Rev. B* **48**, 3404 (1993).

¹¹H. Drulis, Z. G. Xu, J. W. Brill, L. E. De Long, and J.-C. Chou, *Phys. Rev. B* **44**, 4731 (1991).

¹²C. Rossel, O. Pena, H. Schmitt, and M. Sergent, *Physica C* **181**, 363 (1991).

¹³D. N. Zheng, H. D. Ramsbottom, and D. P. Hampshire, *Phys. Rev. B* **52**, 12 931 (1995).

¹⁴J. Guimpel, P. Hoghoj, I. K. Schuller, J. Vanacken, and Y.

- Bruynseraede, *Physica C* **175**, 197 (1991).
- ¹⁵D. Dimos, P. Chaudhari, J. Mannhart, and F. K. LeGoues, *Phys. Rev. Lett.* **61**, 219 (1988).
 - ¹⁶D. R. Clark, T. M. Shaw, and D. Dimos, *J. Am. Ceram. Soc.* **72**, 1103 (1989).
 - ¹⁷L. Cooley, M. Daeumling, T. C. Willis, and D. C. Larbalestier, *IEEE Trans. Magn.* **35**, 2314 (1988).
 - ¹⁸T. Takagi, Y.-M. Chiang, and A. Roshko, *J. Appl. Phys.* **68**, 5750 (1990).
 - ¹⁹C. P. Bean, *Rev. Mod. Phys.* **36**, 31 (1964).
 - ²⁰N. R. Werthamer, E. Helfand, and P. C. Hohenberg, *Phys. Rev.* **147**, 295 (1966).
 - ²¹A. A. Abrikosov, *Zh. Eksp. Teror. Fiz.* **32**, 1442 (1957) [*Sov. Phys. JETP* **5**, 1174 (1957)].
 - ²²K. Kitazawa, S. Uchida, and S. Tanaka, *Physica B* **135**, 505 (1985).
 - ²³K. Kitazawa, A. Katsui, A. Toriumi, and S. Tanaka, *Solid State Commun.* **52**, 459 (1984).
 - ²⁴H. Takagi, M. Naito, S. Uchida, K. Kitazawa, and S. Tanaka, *Solid State Commun.* **55**, 1019 (1985).
 - ²⁵D. N. Zheng, A. M. Campbell, J. D. Johnson, J. R. Cooper, F. J. Blunt, A. Porch, and P. A. Freeman, *Phys. Rev. B* **49**, 1417 (1994).
 - ²⁶B. Batlogg, R. J. Cava, L. F. Schneemeyer, and G. P. Espinosa, *IBM J. Res. Dev.* **33**, 208 (1989).
 - ²⁷Y. Xu, M. Suenaga, A. R. Moodenbaugh, and D. O. Welch, *Phys. Rev. B* **40**, 10 882 (1989).
 - ²⁸Y. Teshurun and A. P. Malozemoff, *Phys. Rev. Lett.* **60**, 2202 (1988).
 - ²⁹A. M. Campbell and J. E. Evetts, *Adv. Phys.* **21**, 199 (1972).
 - ³⁰H. Safar, P. L. Gammel, D. A. Huse, D. J. Bishop, J. R. Rice, and D. M. Ginsberg, *Phys. Rev. Lett.* **69**, 824 (1992).
 - ³¹W. K. Kwok, J. Fendrich, S. Fleshler, U. Welp, J. Downey, and G. W. Crabtree, *Phys. Rev. Lett.* **72**, 1092 (1994).
 - ³²B. Billon, M. Charalambous, J. Chaussy, R. Koch, and R. Liang, *Phys. Rev. B* **55**, R14 753 (1997).
 - ³³E. Zeldov, D. Majer, M. Konczykowski, V. B. Geshkenbein, and V. M. Vinokur, *Nature (London)* **375**, 373 (1995).
 - ³⁴A. Schilling, R. A. Fisher, N. E. Phillips, U. Welp, D. Dasgupta, W. K. Kwok, and G. W. Crabtree, *Nature (London)* **382**, 791 (1996).
 - ³⁵M. Roulin, A. Junod, and E. Walker, *Science* **273**, 1210 (1996).
 - ³⁶K. Ghosh, S. Ramakrishnan, A. K. Grover, Gautam I. Menon, G. Chandra, T. V. C. Rao, G. Ravikumar, P. K. Mishra, V. C. Sahni, C. V. Tomy, G. Balakrishnan, D. Mck Paul, and S. Bhat-tacharya, *Phys. Rev. Lett.* **76**, 4600 (1996).
 - ³⁷R. Cubitt, E. M. Forgan, G. Yang, S. L. Lee, D. McK. Paul, H. A. Mook, M. Yethiraj, P. H. Kes, T. W. Li, A. A. Menovsky, Z. Tarnawski, and K. Mortensen, *Nature (London)* **365**, 407 (1993).
 - ³⁸D. E. Farrell, E. Johnston-Halperin, L. Klein, P. Fournier, A. Kapitulnik, E. M. Forgan, A. I. M. Rae, T. W. Li, M. L. Traw-ick, R. Sasik, and J. C. Garland, *Phys. Rev. B* **53**, 11 807 (1996).
 - ³⁹U. Welp, J. A. Fendrich, W. K. Kwok, G. W. Crabtree, and B. W. Veal, *Phys. Rev. Lett.* **76**, 4809 (1996).
 - ⁴⁰M. Willemin, A. Schilling, H. Keller, C. Rossel, J. Hofer, U. Welp, W. K. Kwok, R. J. Olsson, and G. W. Crabtree, *Phys. Rev. Lett.* **81**, 4236 (1998).
 - ⁴¹D. Babic, J. R. Cooper, J. W. Hodby, and Chen Changkang, *Phys. Rev. B* **60**, 698 (1999).